WOOD RESEARCH
64 (5): 2019
821-832

PREPARATION AND CHARACTERIZATION OF ANTIBACTERIAL FILMS FROM BAMBOO

Ying Guan, Hui Gao, Wenqi Li, Jun Rao, Yuqi Zhang
Anhui Agricultural University
Herfei, China

(Received January 2019)

ABSTRACT

The aim of this research was to prepare lignocellulose films reinforced with chitosan (CS), nano-ZnO (NZO), or nano-TiO_2 (NTD) by casting method. The chemical structures of the films were characterized with FT-IR, which showed no chemical bonds formed but certain interactions among the hydrogen bonds. X-ray diffraction confirmed that the main structure of blend films was unchanged comparing to lignocellulose film. Derivative thermogravimetry (DTG) presented that the residual masses of lignocellulose/chitosan (LCCS) film, lignocellulose/TiO_2 (LCTD) film, and lignocellulose/ZnO (LCZO) film were 23.43%, 19.27%, 27.68% at 700°C, respectively. Ultimate tensile strength and strain to break of all blend films were decreased with addition of CS, NZO, and NTD, respectively. LCCS film was more effective against *Escherichia coli* and *Staphylococcus aureus* than LCTD film and LCZO film. Potential antimicrobial applications in the orthopedic field and perspectives regarding future studies in this field were also considered.

KEYWORDS: Bamboo, chitosan, titanium dioxide, zinc oxide, blend film.

INTRODUCTION

With the depletion of global fossil fuels and the wide concerns about environmental problems, the utilization of renewable resources has attracted more and more attention during recent years (Xia et al. 2016). Due to their unique advantages, such as clean, efficient, safe, and sustainable, bio-based materials were likely to capture new product markets in the future as fossil fuels become less available (Ayoub et al. 2013).

Phyllostachys pubescens is the most widely planted bamboo species in China, it is also the most valuable species with highest economic value. Therefore, the utilization of bamboo as a lignocellulosic raw material is to ease the energy crisis and improve the ecological environment of great importance. It is mainly composed of three natural polymers: cellulose, hemicelluloses, lignin, which accounted for about 90% of its dry weight. Cellulose is a polydisperse linear homopolymer consisting of d-glucose units connected by regio- and enantioselective

-1, 4-glycosidic, which contains three reactive hydroxyl groups at the C-2, C-3 and C-6 atoms (Heize and Liebert 2001). Hemicelluloses are comprised of five carbon sugar, six carbon sugar and other different types of monosaccharides, such as xylose, glucose, mannose, galactose, etc., with 500–3000 sugar units per molecule (Scheller and Ulvskov 2010). The basic skeleton of lignin is phenylpropane, which composed of sinapyl, coniferyl, and p-coumaryl alcohols. Lignin is a complex amorphous polymer with a three-dimensional structure (Hartfield and Vermerris 2001). The three-dimensional network structures of lignocellulosic cell as well as covalent linkages between lignin and polysaccharides make the polymer insoluble in majority of conventional solvents, which limit the potential applications of these abundant renewable resources (Yang et al. 2013).

In the past decade, many studies have focused on the dissolution of natural polymers in ion liquids (ILs), which exhibit a great potential of ILs as solvents (da Costa Lopes et al. 2013). Cellulose was one of the most studied natural polymers proved a high solubility in many kinds of ILs (Zakrzewska et al. 2010). Using different ILs to examine a wide range of carbohydrate solubilities indicates that one of the main benefits of using ILs to dissolve carbohydrates was that ILs can be adjusted to achieve the dissolution or functionalization of these polymers. The current study reported that 1-butyl-3-methylimidazolium chloride (BmimCl) was a potent solvent for cellulose, up to 25 wt. % of cellulose can be dissolved in BmimCl to form a homogeneous solution (Swatloski et al. 2002). Many researchers have been reported that the lignocellulosic biomass can be dissolve in ILs successfully (Brandt et al. 2013).

In recent years, due to its biodegradability, low carbon dioxide release, renewability, low cost, many efforts have been made to develop sustainable composite materials for a variety of industrial purposes (Khalil et al. 2016). Chitosan, an abundant natural polymer, possess antimicrobial activity, wound healing properties and hemostatic activity which makes chitosan-based composites very useful biomedical applications. Among metal oxides nanoparticles, titanium dioxide has been widely studied as coating material for textile fabrics to provide functions such as antibacterial activity (Daoud and Xin 2004). Recently, Martins et al. have prepared the antibacterial nanofibrillated cellulose (NFC)/ZnO nanocomposite coated paper by using a size press machine. This nanocomposite has been tested against Gram-positive (*S. aureus* and *B. cereus*) and Gram-negative (*K. pneumonia*) bacteria (Martins et al. 2013). The aim of this research was to prepare an ecofriendly active film from lignocellulose incorporated with chitosan, TiO_2, ZnO, respectively. The chemical structures of the synthesized films were characterized by FTIR, the phase analyses of the synthesized films were investigated by XRD, and thermo-gravimetric analyses (TGA/DTG) were used to evaluate the thermal stability of prepared films. To determine the synthesized films would have potential to be used as an active packaging, mechanical properties, antibacterial and antioxidant activity of the films were also evaluated.

MATERIALS AND METHODS

Materials

1, 4-dioxane was purchased from Chengdu Ke-Long Chemical Industry Co. Ltd. Hydrochloric acid was provided by Shanghai Zheng-Qi Chemical Industry Co. Ltd. The nano-titanium, nano-zinc oxide, and LB media (include Tryptone, Yeast extract, NaCl) were procured from Aladdin. BmimCl was obtained from institute of chemical physics, Chinese academy of sciences. The model bacteria of *Escherichia coli* (E. coli, the strain of bacteria is ATCC 25922) and *Staphylococcus aureus* (S. aureus, the strain of bacteria is ATCC 25923) were supplied by institute

of biological engineering in Huainan Normal University (Huainan, China). All the reagents used in the experiment were analytical grade and used without any further purification.

Preparation of blend film

The dried bamboo specimens were ground into small pieces, and the 40-60 mesh particles were sifted for further experiment. The bamboo powder was extracted with ethanol/toluene (1:2, v/v) in a Soxhlet apparatus for 6 h and dried in cabinet oven with air circulation for 16 h at 60°C. Then, the extractive-free sample was extracted with 36% HCl/H_2O/1, 4-dioxane (1:5:20, v/v/v) for 1.5 h at 90°C. Afterwards, the extractive-free bamboo material was ball-milled at room temperature for 12.5 h with a rotation speed of 500 rpm.

The pretreated bamboo powder (0.5 g) was added into 9.5 g BmimCl and stirred for 12 h at 110°C under nitrogen atmosphere to dissolve completely. The solution was cast into a tetrafluoroethylene mold and placed in a constant temperature and moisture content chamber (temperature 30°C, moisture content 60%) for 24 h. The film was then removed and placed in a Petri dish filling with distilled water. The residual ionic liquid in the regeneration film was replaced with distilled water. Then, the lignocellulose film was dried under vacuum at 40°C for 24 h. In addition, chitosan (0.01 g), nano-ZnO (0.01 g), and nano-TiO_2 (0.01 g) were added into the mixed solution of bamboo and BmimCL, respectively. Lignocellulose/chitosan (LCCS), lignocellulose/ZnO (LCZO), lignocellulose/TiO_2 (LCTD) films were prepared according to the previous procedures.

FT-IR spectroscopy

The FTIR spectra were obtained on a Nicolei6670 FTIR spectrophotometer, dried samples were using KBr, and their spectra were recorded from 4 000 to 400 cm^{-1} at a resolution of 2 cm^{-1} in the transmission mode.

X-Ray diffraction

XRD measurements were performed using XRD-3 diffractometer (PERSEE, Bei- Jing) by Co Kα radiation and X-ray wavelength of 0.154 nm at 36 kV and 20 mA. Regeneration films were analyzed between 2θ=5° and 40° with the angle size of at 2θ=0.02° speed of 1° min^{-1} at room temperature.

Mechanical property

Mechanical properties of the dry films were examined with an Instron 5565 universal testing machine. Rectangular specimens were cut to 30 × 3 × 0.09 mm and extended at a constant crosshead speed of 10 mm·min^{-1}. And the test temperature was 25°C, the relative humidity was 30%.

Thermal gravimetric analysis

Regeneration films were characterized by TGA analyzer (TG209, Netzsch) under a nitrogen atmosphere. The heating temperature was from 35 to 700°C with the rate of 10°C·min^{-1}. The regeneration films were previously dried at 40°C before performing the TGA analyses.

Antibacterial susceptibility test

The bactericidal activity of the blend films at the same concentrations against *Escherichia coli* (*E. coli*) and *Staphylococcus aureus* (*S. aureus*) were evaluated, respectively. Nutrient agar medium was obtained by dissolving 0.5 g beef broth, 1g NaCl, 1.5 g agar, and 1 g peptone in 100 ml

distilled water. The bacteria were transferred and spread onto the solid surface of the medium. The sample were cut into pieces of 6 mm in diameter and placed in a sterilization pot for 20 min at 121°C, 15 μl of each dilution was placed on LB medium. After incubation for 24 h at 37°C, the inhibition zones were measured and photographed.

RESULTS AND DISCUSSION

FT-IR analysis of the blend film

Many researches have been reported that the band below 600 cm^{-1} was attributed to stretching and bending vibrations of Zn-O bonding, which was observed in the sample of ZnO nanocomposite material. And the stretching vibrations of Ti-O were visible as bands in the range of 400-660 cm^{-1} (Rajbongshi et al. 2015). FTIR spectra of lignocellulose and composite films were present in Fig. 1.

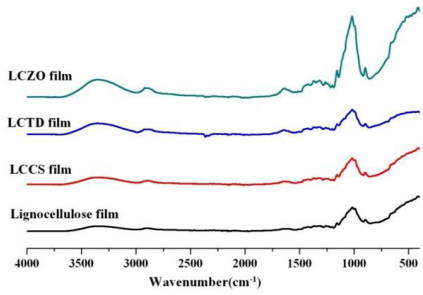

Fig. 1: FTIR spectra of lignocellulose and composite films prepared from ionic liquid solutions.

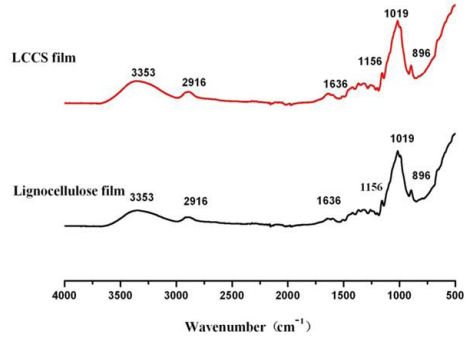

Fig. 2: FTIR spectra of lignocellulose and LCCS films.

From the Fig. 1, the absorption of nano-TiO_2 and nano-ZnO in the mid-infrared region were very weak, and its strong absorption peak in the far-infrared region was not suitable for analyzing by mid-infrared spectroscopy. Therefore, the mid-infrared spectroscopy analyses of LCTD film and LCZO film were not discussed in this research.

From the FTIR spectrum of LCCS film in Fig. 2, the absorption peak at 1156 cm^{-1} was according to the antisymmetric bridge stretching vibration of cellulose and hemicellulose. The band at 1156 cm^{-1} was attributed to the internal standard peak. The spectrum of lignocellulose film showed similar bands to those of LCCS film except for the absorption band at 1538 cm^{-1}, which was characteristic to –NH bending in amides and amines in the chitosan structure (Stefanescu et al. 2012). The characteristic peak of C-H vibrations (2916 cm^{-1}) was ascribed to the cellulose (Janpetch et al. 2016, Ko et al. 2014). The absorption peak at 1636 cm^{-1} was due to C=O and C=C stretching of lignin, FTIR spectrum of LCCS film showed that stretching vibration absorption peak of N-H and O-H at about 3354 cm^{-1} showed some strengthen trend, which indicated interactions were occurred between cellulose and chitosan (Shafei et al. 2011). The specific bands of the β-(1-4) glycoside bridge at 896 cm^{-1}, as well as C-O-C stretching vibration in the pyranose at 1156 cm^{-1} were also clearly present in the spectra (Rajbongshi et al. 2015, Caldeira et al. 2013).

XRD of the blend film

XRD patterns of original (pretreated bamboo powder) and lignocellulose film (prepared from ionic liquid solutions) were present in Fig. 3, which can be seen that the lignocellulose film had a wide diffraction peak near 19.24° and the diffraction peak of cellulose I disappears at 101, 002 and 040 crystal planes compared with the XRD pattern of the original bamboo material. This phenomenon indicating there was a crystal form transformation during the dissolution and regeneration process.1 X-ray diffraction profiles of LCCS, LCTD, LCZO film and lignocellulose films were shown in Fig. 4, which were displayed more information about the crystalline phase in these samples. Obviously, the XRD patterns of LCZO film showed well-defined peaks at 2θ = 19.24°, which were assigned to cellulose. In addition to the main diffraction peak at 2θ = 19.24°, the LCZO film showed three small peaks between 30° and 40°, which were related to the ZnO crystallite (Qin et al. 2016, Youssef et al. 2016).

After dissolution and regeneration of LCTD film, a broad peak at 2θ = 19.24° and a narrow peak at 2θ = 24.2° were present in the XRD profile of the LCTD film. There were obtained by regenerated from distilled water. The narrow peak was attributed to the lattice planes of TiO_2 inorganic additives (Qin et al. 2016). When the blend films were regenerated from ionic liquid solutions, the typical diffraction profiles of native chitosan (2θ = 11.2° and 20.04°) were still exists with weaker intensity indicating that the native crystal structure of chitosan was reconstructed but suffers a remarkable decrease in crystallinity.

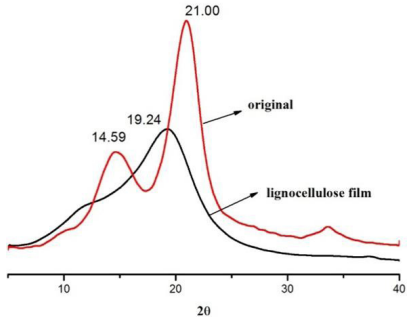

Fig. 3: XRD patterns of original (pretreated bamboo powder) and lignocellulose film (prepared from ionic liquid solutions).

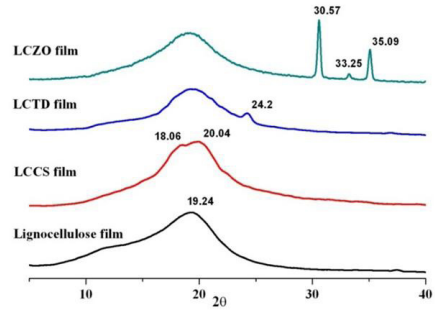

Fig. 4: XRD patterns of blend films regenerated from ionic liquid solutions.

On the other hand, a peak at 2θ = 19.24° and no peak at 14.59° were obtained in the diffraction pattern of the lignocellulose film. This result was consistent with a transformation from cellulose I to cellulose II (Zhao et al. 2009, Hameed and Guo 2010). No peak was shown at 2θ = 11.2° in the XRD profile of the LCCS film, which could be explained by inhibition of the crystallization of chitosan. This was due to the formation of hydrogen bonds between chitosan and cellulose, and thus miscibility between polymers (Luo et al. 2008, Xu et al. 2005).

Mechanical property of the blend film

The mechanical properties of regenerated films can be seen in Tab. 1 and Fig. 5. The mechanical properties of the films were also greatly influenced by the addition of blend materials (chitosan, nano-zinc oxide, nano titanium dioxide). The tensile stress of the lignocellulose film was 148.3 MPa, while that of LCCS film, LCTD film and LCZO film were 102.6, 143.6, and

94.5 MPa, respectively (Shankar et al. 2015). The elongation at break for lignocellulose film was higher than that of LCCS, LCTD, and LCZO films.

Tab. 1: Mechanical property of the blend films.

Samples	Lignocellulose film	LCCS film	LCTD film	LCZO film
Tensile stress (MPa)	148.3	102.6	143.6	94.5
Elongation at break (%)	12.22	10.05	4.70	2.39

The important information of the internal structure of materials was also provided by the mechanical properties of the composite materials, which were strongly influenced by their microstructure (Xiong et al. 2015). The results of the mechanical properties of the LCCS film indicated that the extensibilities of the films were reduced by adding of chitosan to the blend mixture and obtained more fragile products. Weak tensile properties of chitosan were the primary cause of decreased elongation (Masoomi et al. 2015). The changes in tensile properties showed that structural changes were caused by incorporation of ZnO into lignocellulose films. It was known that the mechanical properties of the films were determined by polymer matrix between intermolecular and intra-molecular interactions (Shankar et al. 2015).

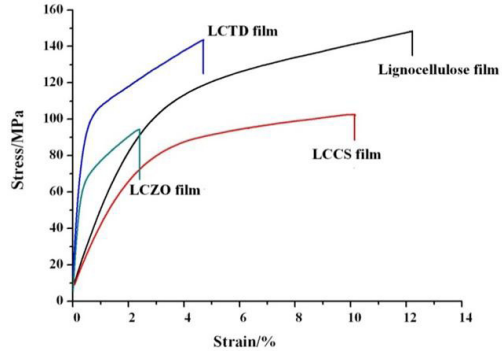

Fig. 5: Stress–strain behavior for lignocellulose, LCCS, LCTD, and LCZO films.

Thermal stability of the blend film

Thermo-gravimetric analyses were carried out to evaluate their thermal stabilities and degradation profiles (Fig. 6a, b). The TGA results exhibited a three-step thermal degradation pattern of films in Fig. 6a. The films showed two mass losses, and the volatilization of water was at around 100°C and 200°C. The main mass was occurred between 290°C and 330°C, which were ascribed to the decomposition of the lignocelluloses. Fig. 6b displayed the effects of the films contents on the maximum degradation temperature of the blend films.

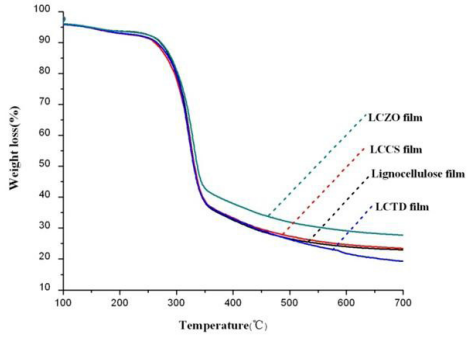

Fig. 6a: Thermogravimetric plot, TGA, for lignocellulose, LCCS, LCTD, and LCZO films.

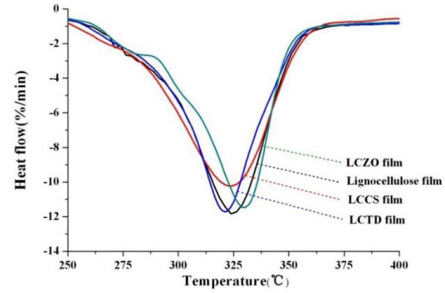

Fig. 6b: DTG curves of lignocellulose, LCCS, LCTD, and LCZO films.

As shown in Tab. 2, the lignocellulose film exhibited the maximum degradation temperature at 324.3°C, whereas the temperatures were 325.6°C, 321.7°C, and 329.3°C for LCCS film, LCTD film, and LCZO films, respectively.

Tab. 2: The data analysis of TGA curves.

Samples	T_{onset} (°C)	T_{max} (°C)	R_{max} (%/min)	M_{ass} (%)
Lignocellulose film	295.70	324.30	-11.84	22.95
LCCS film	296.40	325.60	-10.98	23.43
LCTD film	295.30	321.70	-11.67	19.27
LCZO film	299.10	329.30	-11.50	27.68

T_{onset} - temperature that material begins to degrade, T_{max} - temperature that material degrades the fastest, R_{max} - maximum rate of decomposition of the material. M_{ass} indicated the residual mass of the material.

The results suggested that the thermal stability of the LCZO film was the best among all samples, and the thermal stabilities of the lignocellulose films were decreased with addition of the nano-TiO_2 (Qin et al. 2016). The thermal stability of lignocellulose was increased by the addition of chitosan, and the thermal degradation was slowed down. The results indicated that the interactions between the hydroxyl groups of cellulose and the amino groups of chitosan were established in the ionic liquid solution (Stefanescu et al. 2012).

It was found that the thermal stability of lignocellulose film was slightly enhanced by the incorporation of ZnO into lignocellulose film. It identified the synergy between ZnO and lignocellulose. The weight loss of lignocellulose film was higher than that of LCCS film and LCZO film, but lower than that of the LCTD film. This behavior of the LCCS film might be explained by the interactions of hydrogen bond between chitosan and cellulose, which might disrupt the crystalline structures of the blend film. Compared with the presence of more crystalline regions, the more amorphous blend has the ability to remain more water.

Antibacterial activity of the blend film

Fig. 7a - Fig. 7d showed the antibacterial effect of bamboo regeneration film on *E. coli* and *S. aureus*. The antimicrobial susceptibility disk was positive control, and the pure cellulose film was negative. From Fig. 7a - Fig. 7d there was no obvious inhibition zone of lignocellulose

film. The reason of this phenomenon was that the decrease of the lignin was occurred on the dissolution and regeneration. In order to enhance the antibacterial properties of films, CS, NZO, NTD were added in the blending material. As can be seen from the Fig. 7c and Fig. 7d, obvious inhibition zone was presented in the blend film, and it had different antibacterial effects due to the different materials added.

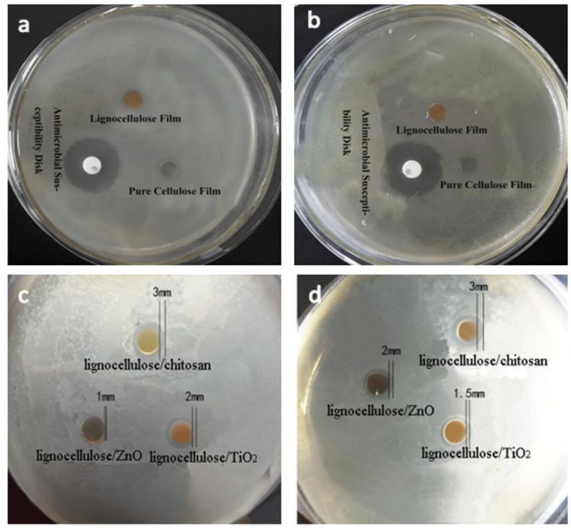

Fig. 7: Antibacterial activity against E. coli (a, c) and S. aureus (b, d).

The size of inhibition zone of film was shown in Tab. 3. Three kinds of blend films of E. coli inhibition zone as follow: LCCS film> LCTD film> LCZO film. The antibacterial activity of LCZO film against S. aureus was higher than that of LCTD film, but lower than LCCS film.

Tab. 3: Inhibition zone of the blend films against E. coli and S. aureus.

Samples	Diameter of zone (mm)		
	LCCS film	LCTD film	LCZO film
E. coli	3.0	2.0	1.0
S. aureus	3.0	1.5	2.0

Early research indicated the antimicrobial potential chitosan dated from the 1980-1990s (Goy et al. 2009). Nowadays, several mechanisms were proposed for the antimicrobial activity by chitosan. In one mechanism, a polymer film can be formed by the chitosan on the surface of the cell, which prevents nutrients from entering the cell (Zheng and Zhu 2003). Another mechanism involves the combination of chitosan and DNA to inhibit RNA synthesis. It has been suggested that chitosan is released from the cell wall of fungal pathogens through the plant host hydrolytic enzymes chitosan penetrates the nuclei of fungus and interferes with the synthesis of RNA and protein. The organism may be weakened by both its own chitosan and host plant antitoxin induced by the released chitosan (Liu et al. 2001).

The possible mechanisms for antimicrobial activity of ZnO were: (1) a few studies have suggested that the main reason for the antibacterial function might be from the damage on cell membrane activity. (2) It has also been reported that ZnO can be activated by UV and visible light

to produce highly reactive oxygen species such as OH-, H_2O_2, and O^{2-}. The induction of reactive oxygen is a strong oxidizing agent harmful to bacterial cells (Xie et al. 2011). Nano-titanium dioxide is the most commonly used photocatalytic antibacterial agent. There are two different antibacterial mechanisms. One is the direct effect of ultraviolet light on the activation of titanium dioxide and cells, that is, photogenerated electrons and photogenerated holes directly reaction of the cell membrane, cell wall or cell composition. The other is the ultraviolet light to stimulate the indirect reaction of titanium dioxide and cells (Xie et al. 2011, Kubacka et al. 2014). It was found that the antibacterial activity of LCZO film against *S. aureus* was higher than *E. coli.* It could be explained that the more positive charges on the cell surface of a *S. aureus* interact more affected by ZnO compare with *E. coli*. In addition, ZnO also inhibited the protein fiber produced by coagulase of S. aureus (Janpetch et al. 2016). The antibacterial activity of LCCS film against *S. aureus* and *E. coli* was higher than that of LCZO and LCTD films, which might be due to the different antibacterial mechanism of three blend films.

CONCLUSIONS

To increase the antibacterial activity and improve the application of lignocellulose, nano-ZnO, nano-TiO^2, and chitosan were added into lignocellulose. The method provides valuable insights into developing antibacterial materials with film-forming capacity. The blend films exhibited remarkable bacteriostatic ability against *S. aureus* and *E. coli*. The antibacterial properties of blend films against *E. coli* were found as follows: lignocellulose/chitosan blend film > lignocellulose/TiO^2 blend film > lignocellulose /ZnO blend film. The antibacterial properties of three kinds of films against *Staphylococcus aureus* were found as follows: lignocellulose/chitosan blend film > lignocellulose/ ZnO blend film > lignocellulose/TiO^2 blend film. Ultimate tensile strength (UTS) and strain at break (STB) of all blend films were decreased with addition of chitosan (CS), nano-ZnO (NZO), and nano-TiO^2 (NTD) into the lignocellulose, respectively. Thermal stabilities of LCCS film and LCZO film were better than that of lignocellulose film, while the thermal stability of LCTD film was slightly lower than that of lignocellulose film. FTIR spectra of blend film suggested that no chemical bond was formed but certain interactions were coming from the hydrogen bonds. X-ray diffraction confirmed that the main structure of blend films was unchanged comparing to lignocellulose film. Overall, the blend films have great potential use as fresh food packaging, but there are a number of questions remained to be answered before a firm conclusion could be drawn.

ACKNOWLEDGEMENTS

This work was supported by the Anhui Postdoctoral Science Foundation Grant (2017B157), Introduction and Stability Talent Project of Anhui Agricultural University (yj2016-10), Innovation and Entrepreneurship Training Project of Anhui University Student (201810364090) and China Postdoctoral Science Foundation Grant (2016M601996).

REFERENCES

1. Ayoub, A., Venditti, R.A., Pawlak, J.J., Sadeghifar, H., Salam, A., 2013: Development of an acetylation reaction of switchgrass hemicellulose in ionic liquid without catalyst. Industrial Crops and Products 44: 306-314.

2. Brandt, A., Gräsvik, J., Hallett, J.P., Welton, T., 2013: Deconstruction of lignocellulosic biomass with ionic liquids. Green Chemistry 15(3): 550-583.
3. Caldeira, E., Piskin, E., Granadeiro, J., Silva, F., Gouveia, I.C., 2013: Biofunctionalization of cellulosic fibres with l-cysteine: Assessment of antibacterial properties and mechanism of action against Staphylococcus aureus and Klebsiella pneumonia. Journal of Biotechnology 168(4): 426-435.
4. Da Costa Lopes, A.M., João, K.G., Morais, A.R.C., Bogel-Łukasik, E., Bogel-Łukasik, R., 2013: Ionic liquids as a tool for lignocellulosic biomass fractionation. Sustainable Chemical Processes 1(1): 3-34.
5. Daoud, W.A., Xin, J.H., 2004: Low temperature sol-gel processed photocatalytic titania coating. Journal of Sol-Gel Science and Technology 29(1): 25-29.
6. Goy, R.C., Britto, D.D., Assis, O.B.G., 2009: A Review of the Antimicrobial Activity of Chitosan, Polímeros: Ciência e Tecnologia 19(3): 241-247.
7. Hameed, N., Guo, Q., 2010: Blend films of natural wool and cellulose prepared from an ionic liquid. Cellulose 17(4): 803-813.
8. Hatfield, R., Vermerris, W., 2001: Lignin formation in plants. The dilemma of linkage specificity. Plant Physiology 126(4):1351-1357.
9. Heinze, T., Liebert, T., 2001: Unconventional methods in cellulose functionalization. Progress in Polymer Science 26(9): 1689-1762.
10. Janpetch, N., Saito, N., Rujiravanit, R., 2016: Fabrication of bacterial cellulose-ZnO composite via solution plasma process for antibacterial applications. Carbohydrate Polymers 148: 335-344.
11. Khalil, H.P.S.A., Saurabh, C.K., Adnan, A.S., Fazita, M.R.N., Syakir, M.I., Davoudpour, Y., Rafatullah, M., Abdullah, C.K., Haafiz, M.K.M., Dungani, R., 2016: A review on chitosan-cellulose blends and nanocellulose reinforced chitosan biocomposites: Properties and their applications. Carbohydrate Polymers 150: 216-226.
12. Ko, H.U., Mun, S., Min, S.K., Kim, G.W., Kim, J., 2014: Fabrication of cellulose ZnO hybrid nanocomposite and its strain sensing behavior. Materials 7(10): 7000-7009.
13. Kubacka, A., Diez, M.S., Rojo, D., Bargiela, R., Ciordia, S., Zapico, I., 2014: Understanding the antimicrobial mechanism of TiO_2-based nanocomposite films in a pathogenic bacterium. Scientific Reports 4: 4134-4142.
14. Liu, X.F., Guan, Y.L., Yang, D.Z., Li, Z., Yao, K.D., 2001: Antibacterial Action of Chitosan and Carboxymethylated Chitosan. Journal of Applied Polymer Science 79(7): 1324-1335.
15. Luo, K., Yin, J., Khutoryanskaya, O.V., Khutoryanskiy, V.V., 2008: Mucoadhesive and elastic films based on blends of chitosan and hydroxyethylcellulose. Macromolecular Bioscience 8(2): 184-192.
16. Martins, N.C.T., Freire, C.S.R., Neto, C.P., Silvestre, A.J.D., Causio, J., Baldi, G., 2013: Antibacterial paper based on composite coatings of nanofibrillated cellulose and ZnO. Colloids and Surfaces A: Physicochemical and Engineering Aspects 417: 111-119.
17. Masoomi, M., Tavangar, M., Razavi, S.M.R., 2015: Preparation and investigation of mechanical and antibacterial properties of poly(ethylene terephthalate)/chitosan blend. RSC Advances 5(96): 79200–79206.
18. Qin, Y., Zhang, S.L., Yu, J., Yang, J., Xiong, L., Sun, Q.J., 2016: Effects of chitin nano-whiskers on the antibacterial and physicochemical properties of maize starch films. Carbohydrate Polymers 147: 372-378.

19. Rajbongshi, B.M., Samdarshi, S.K., Boro, B., 2015: Multiphasic bi-component TiO_2–ZnO nanocomposite: synthesis, characterization and investigation of photocatalytic activity under different wavelengths of light irradiation. Journal of Materials Science: Materials in Electronics 26(1): 377-384.
20. Shafei, A.E., Abou-Okeil, A., 2011: ZnO/carboxymethyl chitosan bionano-composite to impart antibacterial and UV protection for cotton fabric. Carbohydrate Polymers 83(2): 920-925.
21. Scheller, H.V., Ulvskov, P., 2010: Hemicelluloses, Annual Review of Plant Biology 61: 263-289.
22. Shankar, S., Teng, X., Li, G., Rhim, J.W., 2015: Preparation, characterization, and antimicrobial activity of gelatin/ZnO nanocomposite films. Food Hydrocolloids 45: 264-271.
23. Stefanescu, C., Daly, W.H., Negulescu, I.I., 2012: Biocomposite films prepared from ionic liquid solutions of chitosan and cellulose. Carbohydrate Polymers 87(1): 435-443.
24. Swatloski, R.P., Spear, S.K., Holbrey, J.D., Rogers, R.D., 2002: Dissolution of Cellose with Ionic Liquids. Journal of the American Chemical Society 124(18): 4974-4975.
25. Xia, G.M., Wan, J.Q., Zhang, J.M., Zhang, X.Y., Xu, L., Wu, J., He, J.S., Zhang, J., 2016: Cellulose-based films prepared directly from waste newspapers via an ionic liquid. Carbohydrate Polymers 151: 223-229.
26. Xie, Y.P., He, Y.P., Irwin, P.L., Jin, T., Shi, X.M., 2011: Antibacterial activity and mechanism of action of zinc oxide nanoparticles against campylobacter jejuni. Applied and Environmental Microbiology 77(7): 2325-2331.
27. Xiong, F.Q., Zhou, L., Qian, L.C., Liu, S.Q., 2015: Effects of pretreatment methods using various 1,4-dioxane concentrations on the performance of lignocellulosic films of Eucalyptus citriodora. BioResources 10(1): 1149-1161.
28. Xu, Y.X., Kim, K.M., Hanna, M.A., Nag, D., 2005: Chitosan–starch composite film: preparation and characterization. Industrial Crops and Products 21(2): 185-192.
29. Yang, D., Zhong, L.X., Yuan, T.Q., Peng, X.W., Sun, R.C., 2013: Studies on the structural characterization of lignin, hemicelluloses and cellulose fractionated by ionic liquid followed by alkaline extraction from bamboo. Industrial Crops and Products 43: 141-149.
30. Youssef, A.M., El-Sayed, S.M., El-Sayed, H.S., Salama, H.H., Dufresne, A., 2016: Enhancement of Egyptian soft white cheese shelf life using a novel chitosan/carboxymethyl cellulose/zinc oxide bionanocomposite film. Carbohydrate Polymers 151: 9-19.
31. Zakrzewska, M.E., Łukasik, E.B., Łukasik, R.B., 2010: Solubility of Carbohydrates in Ionic Liquids. Energy & Fuels 24(2): 737-745.
32. Zhao, Q., Yam, R.C.M., Zhang, B.Q., Yang, Y.K., Cheng, X.J., Li, R.K.Y., 2009: Novel all-cellulose ecocomposites prepared in ionic liquids. Cellulose 16(2): 217-226.
33. Zheng, L.Y., Zhu, J.G., 2003: Study on antimicrobial activity of chitosan with different molecular weights. Carbohydrate Polymers 54(4): 527-530.

*Ying Guan, Hui Gao, Wenqi Li, Jun Rao, Yuqi Zhang
School of Forestry and Landscape
Anhui Agricultural University
130 Changjiangxilu
Hefei, China
*Corresponding Author: Xiaomi1231@163.Com